Marquette University
e-Publications@Marquette

Biomedical Engineering Faculty Research and Publications

Biomedical Engineering, Department of

Depleted Energy Charge and Increased Pulmonary Endothelial Permeability Induced by Mitochondrial Complex I inhibition are Mitigated by Coenzyme Q$_1$ in the Isolated Perfused Rat Lung

Robert D. Bongard
Medical College of Wisconsin

Ke Yan
Medical College of Wisconsin

Raymond G. Hoffmann
Medical College of Wisconsin

Said H. Audi
Marquette University, said.audi@marquette.edu

Xiao Zhang
Marquette University, xiao.zhang@marquette.edu

See next page for additional authors

Authors

Robert D. Bongard, Ke Yan, Raymond G. Hoffmann, Said H. Audi, Xiao Zhang, Brian J. Lindemer, Mary I. Townsley, and Marilyn P. Merker

Depleted Energy Charge and Increased Pulmonary Endothelial Permeability Induced By Mitochondrial Complex I Inhibition Are Mitigated By Coenzyme Q₁ in the Isolated Perfused Rat Lung

Robert D. Bongard
Department of Pulmonary Medicine, Medical College of Wisconsin
Milwaukee, WI
Ke Yan
Department of Biostatistics, Medical College of Wisconsin
Milwaukee, WI
Raymond G. Hoffmann
Department of Biostatistics, Medical College of Wisconsin
Milwaukee, WI
Said H. Audi
Department of Biomedical Engineering, Marquette University
Milwaukee, WI
Xiao Zhang
Department of Biomedical Engineering, Marquette University
Milwaukee, WI
Brian J. Lindemer
Department of Anesthesiology, Medical College of Wisconsin
Milwaukee, WI

Mary I. Townsley

Departments of Physiology and Medicine, University of South Alabama
Mobile, AL

Marilyn P. Merker

Department of Anesthesiology, Medical College of Wisconsin
Department of Pharmacology/Toxicology, Medical College of Wisconsin
Zablocki VAMC,
Milwaukee, WI

Abstract

Mitochondrial dysfunction is associated with various forms of lung injury and disease that also involve alterations in pulmonary endothelial permeability, but the relationship, if any, between the two is not well understood. This question was addressed by perfusing the isolated intact rat lung with a buffered physiological saline solution in the absence or presence of the mitochondrial complex I inhibitor rotenone (20 uM). As compared to control, rotenone depressed whole lung tissue ATP from 5.66 ± 0.46 (SEM) to 2.34 ± 0.15 (SEM) $\mu mol \cdot gram^{-1}$ dry lung, with concomitant increases in the ADP:ATP and AMP:ATP ratios. Rotenone also increased lung perfusate lactate (from 12.36 ± 1.64 (SEM) to 38.62 ± 3.14 $\mu mol \cdot 15\ min^{-1}$ perfusion$\cdot gm^{-1}$ dry lung) and the lactate:pyruvate ratio, but had no detectable impact on lung tissue GSH:GSSG redox status. The amphipathic quinone, coenzyme Q_1 (CoQ$_1$; 50 µM) mitigated the impact of rotenone on the adenine nucleotide balance, wherein mitigation was blocked by NAD(P)H:quinone oxidoreductase 1 (NQO1) or mitochondrial complex III inhibitors. In separate studies, rotenone increased the pulmonary vascular endothelial filtration coefficient (K_f) from 0.043 ± 0.010 (SEM) to 0.156 ± 0.037 (SEM) ml$\cdot min^{-1} \cdot$cm $H_2O^{-1} \cdot gm^{-1}$ dry lung weight, and CoQ$_1$ protected against the effect of rotenone on K_f. A second complex I inhibitor, piericidin A, qualitatively reproduced the impact of rotenone on K_f and the lactate/pyruvate ratio. Taken together, the observations imply that pulmonary endothelial barrier integrity depends on mitochondrial bioenergetics as reflected in lung tissue ATP levels and that compensatory activation of whole lung glycolysis cannot protect against pulmonary endothelial hyperpermeability in response to mitochondrial blockade. The study further suggests that low molecular weight

amphipathic quinones may have therapeutic utility in protecting lung barrier function in mitochondrial insufficiency.

Keywords: Pulmonary endothelial permeability, pulmonary endothelium, quinone, mitochondrial electron transport complex I, perfused lung, pulmonary endothelial filtration coefficient (K_f)

Introduction

Studies in the isolated perfused lung have revealed that ~80 – 85% of total lung ATP is derived from mitochondrial respiration [1]. Pro-oxidant and other pathophysiological stresses target components of lung mitochondria, including mitochondrial DNA (mtDNA) itself, mitochondrial complex I and other complexes, and the tricarboxylic acid cycle enzyme aconitase [2-6]. Mitochondrial bioenergetic dysfunction arising from these and other lesions has been implicated in various forms of clinical and experimental lung injury [7-16]. While mitochondrial dysfunction is an all-purpose term for a panoply of possible adverse effects on mitochondrial respiration and other mitochondrial functions, a key readout, that may also underlie certain manifestations of lung injury, is impairment of ATP generating capacity [9, 16-21].

Acute lung injury is characterized by increased permeability of the pulmonary endothelial barrier followed by accumulation of protein-enriched fluid in the airspaces and interstitium and impairment of gas exchange [22]. Yet studies manipulating lung mitochondrial bioenergetics as a means to discern its contribution to pulmonary endothelial function have focused primarily on metabolic rather than barrier function, with pulmonary edema used mostly as a toxicity endpoint [23, 24]. The latter studies also involved nearly complete dissipation of mitochondrial ATP generation, e.g., blockade of the terminal chain component, cytochrome oxidase, or use of mitochondrial electron transport uncouplers, and thus did not address a perhaps more likely pathophysiological scenario involving partial impairment at upstream mitochondrial targets. For example, mitochondrial complex I activity is depressed by ~60% in lungs of rats breathing elevated O_2 (85% O_2 for 48 hrs) compared to those in room air, with no detectable effects on complexes III or IV [2]. While the functional impact of the effect on complex I activity was not

specifically investigated, there was no discernible pulmonary edema resulting from the hyperoxic exposure, as reflected in lung wet-to-dry weight ratios [2]. On the other hand, in rabbits exposed to 100% O_2 for 48 hours, while there was also little change in lung water or arterial blood gases in the intact animal, the pulmonary endothelial filtration coefficient (K_f) increased, portending compromised endothelial barrier integrity [25]. Thus, we asked whether there could be a link between mitochondrial complex I activity blockade, mitochondrial function reflected as diminished ATP generation and pulmonary endothelial barrier function.

To address this question, acute exposure to the classical complex I inhibitor, rotenone, was used to induce complex I blockade in the perfused rat lung [26]. Rotenone was selected because our previous studies in this preparation revealed that it caused nearly complete blockade of complex I and depression of whole lung oxygen consumption with no detectable impact on complexes III and IV [2, 27]. To determine the impact of rotenone on lung ATP levels and energy charge, lung tissue adenine nucleotides (ATP, ADP and AMP) were measured. Measurements of lung lactate and pyruvate efflux were also included to evaluate glycolytic activity and lung tissue cytosolic redox status. Finally, the rotenone effect on lung vascular endothelial permeability was measured as the pulmonary endothelial filtration coefficient (K_f) [22].

Complex I inhibition has the advantage in that it provides a convenient model of the mitochondrial response in the hyperoxia-exposed rat lung, wherein downstream electron transport complexes remain open as electron acceptors [2]. This allows for the possibility of restoration of mitochondrial electron transport given the appropriate electron donor or substrate. One possible donor is exemplified by low molecular weight amphipathic hydroquinones that shuttle reducing equivalents from cytosolic NAD(P)H to complex III, effecting a so-called bypass of a complex I block (Scheme 1) [28-30]. This is proposed as a mechanism underlying the therapeutic effect of quinones in treatment of neurological and other diseases arising from mitochondrial genetic disorders, in experimental complex I dysfunction or coenzyme Q_{10} deficiencies in other organs and cell types [28-32]. However, quinones as substrates for reactivation of mitochondrial

electron transport and restoration of mitochondria-dependent lung function have not been considered.
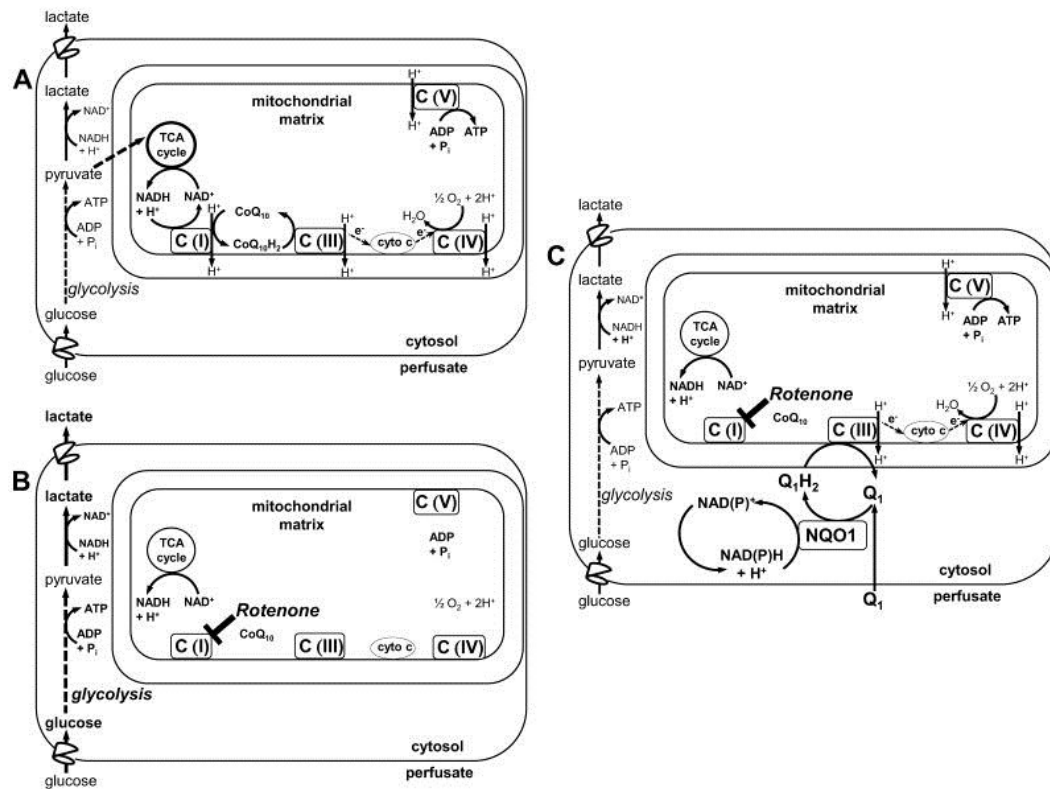
Scheme 1 **Quinone-mediated mitochondrial electron transport complex I bypass**

A. The mitochondrial electron transport chain under physiological conditions, where C(I), C(III), C(IV) and C(V) represent complexes I, III, IV and V, and with the physiological quinone electron acceptor, CoQ_{10}, and its reduced form, $CoQ_{10}H_2$. **B.** Rotenone inhibits electron transport at C(1), blocking transfer of electron to CoQ_{10} and thus to C(III), preventing generation of the proton gradient across the mitochondrial inner membrane, depolarizing the mitochondrial membrane potential ($\Delta\Psi_m$) and depressing ATP production. Compensatory activation of glycolysis increases lung lactate generation as a reflection of increased cytosolic NADH levels. **C.** When the exogenous amphipathic quinone (Q_1) is present, it freely enters the lung tissue, where it is reduced via cytosolic NQO1 at the expense of the endogenous electron donor, NAD(P)H. The reduced hydroquinone form, Q_1H_2, enters the mitochondria and transfers the reducing equivalents gained in the cytosol to C(III), thereby restoring mitochondrial electron transport, proton pumping, $\Delta\Psi_m$ and ATP generation. The reoxidized quinone (Q_1) returns to the cytosol to repeat the cycle. Thus, the Q_1-Q_1H_2 redox pair acts to shuttle electrons from cytosolic NAD(P)H to C(III).

CoQ_1 was selected as the candidate quinone because we have previously studied its redox metabolism on passage through the

isolated perfused rat lung. CoQ_1 freely diffuses from the perfusate into the lung tissue and is reduced to its hydroquinone form (CoQ_1H_2) via cytosolic NAD(P)H quinone oxidoreductase 1 (NQO1) [2]. The CoQ_1H_2 produced crosses the mitochondrial membrane to act as an electron donor at mitochondrial electron transport complex III [2]. Thus, since the CoQ_1-CoQ_1H_2 redox pair undergoes all the steps that theoretically would be needed to effect a complex I bypass in the isolated perfused lung, we hypothesized that CoQ_1 administration would restore mitochondrial bioenergetics, exemplified as ATP generation, and protect the pulmonary endothelial barrier from complex I blockade induced hyperpermeability, should it occur.

Materials and Methods

Materials

2,3-dimethoxy-5-methyl-6-(3-methyl-2-butenyl)-1,4-benzoquinone (coenzyme Q_1, hereafter referred to as CoQ_1) was purchased from Sigma. Bovine serum albumin (BSA) was purchased from Equitech-Bio Inc. Lactate and pyruvate assay kits were obtained from BioVision. All other chemicals, unless otherwise noted, were purchased from Sigma.

Animals

Male Sprague-Dawley rats (Charles River) were housed in room air with free access to food and water. The animal protocol was approved by the Institutional Animal Care and Use Committee (IACUC) of the Zablocki VAMC, Milwaukee, WI USA 53295.

Isolated perfused lung

Rats were anesthetized with pentobarbital sodium (40 mg/kg body wt. i.p.), the chest opened and heparin (0.7 IU/g body wt.) injected into the right ventricle. The lung and heart were removed from the chest en bloc and suspended from a ventilation-perfusion system without (n = 36) or with (n = 39) a calibrated force transducer in place. The lung was ventilated (40 breaths per minute) with a gas mixture containing 15% O_2, 6% CO_2, balance N_2, with end-inspiratory

and end-expiratory pressures of 8 and 3 cm H_2O, respectively. The lung was perfused (0.03 ml·min^{-1}·gram^{-1} body weight) with a physiologic salt solution containing (in mM) 4.7 KCl, 2.51 $CaCl_2$, 1.19 $MgSO_4$, 2.5 KH_2PO_4, 118 NaCl, 25 $NaHCO_3$, 5.5 glucose and 5% bovine serum albumin. The perfusate was maintained at 37°C and equilibrated with the same gas mixture used for ventilation, resulting in perfusate PO_2, PCO_2 and pH of ~105 Torr, 40 Torr and 7.4, respectively. An initial volume of perfusate (~40 ml) was flushed through the lung and discarded, after which time the lung was perfused from a recirculating reservoir containing fresh perfusate. During the initial 10 minutes of recirculation, the venous effluent pressure (P_v) was held at atmospheric pressure, allowing time for the pulmonary arterial pressure (P_a) to stabilize. P_a was referenced to atmospheric pressure at the level of the left atrium and monitored continuously during the course of the experiment.

Following the 10 minute stabilization period, the perfused lungs entered one of two protocols, each described below. In the first protocol, lungs were flash frozen in liquid N_2 for measurements of adenine nucleotides and oxidized (GSSG) and reduced (GSH) forms of glutathione. In the second protocol, pulmonary endothelial permeability was measured as the pulmonary endothelial filtration coefficient (K_f) [22]. In both protocols, samples of pulmonary venous effluent were collected and flash frozen in liquid N_2 for measurements of perfusate lactate and pyruvate levels. All biochemical measurements were normalized to one gram of dry lung weight.

Protocol 1: Lung Adenine Nucleotides, GSH and GSSG

Following a 10 minute stabilization period of lung perfusion, the perfusion pump was briefly halted, the reservoir emptied and refilled with 35 ml fresh perfusate containing vehicle only, rotenone (20 M), rotenone + CoQ$_1$ (50 µM), CoQ$_1$ alone (50 µM), rotenone + CoQ$_1$ + dicumarol (400 µM), or rotenone + CoQ$_1$ + antimycin A (3.6 µM). We have previously shown that at these concentrations, rotenone and CoQ$_1$ do not cause any detectable changes in lung hemodynamics or wet:dry weight ratios [2].

The pump was restarted and the first 10 ml of pulmonary venous effluent was discarded, after which the remaining perfusate

was recirculated through the pulmonary circulation for 15 minutes. After 15 minutes, a 1 ml perfusate sample was collected from the reservoir, flash frozen in liquid N_2 and stored at $-80°C$ for measurement of lactate and pyruvate. Perfusion was halted, the lung quickly cut away from the heart and connective tissue, weighed, flash frozen in liquid N_2, lyophilized to a constant weight, reweighed and ground to a powder, which was dispensed into weighed samples of ~25 mg for storage at $-80°C$.

Adenine nucleotides were extracted from the lung powder samples by addition of 5% perchloric acid (750 µl) followed by centrifugation (10,000 × g, 5 min, 4°C) and neutralization of 500 µl of supernatant with 400 µl K_2HPO_4 (1M). Sixty (60) µl of the extract was mixed with 75 µl of potassium phosphate buffer (64.35 mM, pH 6.0) containing 2.57 mM tetrabutylammonium hydrogen sulfate (2.57 mM), the latter solution being the initial HPLC mobile phase. The solution was filtered through a Nalgene 0.2 µm pore size cellulose acetate syringe filter (Nalge Nunc International, Rochester, NY) prior to injection onto the HPLC system. The HPLC system and mobile phase were as previously described, with the difference being substitution of a Phenomenex Kenetix C18 column (2.6 µm particle size, 100 × 4.6 mm) [33].

The adenine nucleotides were quantified against standards prepared for each experiment, and the values normalized to 1 gm dry lung powder, based on the weights of the individual lung powder fractions used for each individual extraction. The adenylate energy charge was then calculated as = (ATP + ½ ADP)/(ATP + ADP + AMP) [34, 35].

GSSG and GSH glutathione were extracted from the lung powder samples by addition of 2.5% ice cold sulfosalicylic acid containing 0.2% Triton X-100 (final concentration of lung powder, 13.5 mg per ml extraction solution). The extraction mixture was centrifuged (10,000 × g for 5 min at 4°C) and the resulting supernatant diluted 1:10 in 0.1 M sodium phosphate buffer (pH = 7.4) for determination of GSSG and GSH, using the 5,5'-dithio-bis-(2-nitrobenzoic acid)-GSSG reductase recycling assay [36-38].

Protocol 2: Pulmonary Endothelial Permeability (K*f*)

The perfused lungs were suspended from a calibrated force displacement transducer (Model FT03, Grass Instruments) and lung weight was monitored continuously. Following a 10 min stabilization period with P_v set at atmospheric pressure, the perfusate pump was stopped. The reservoir was emptied, then refilled with 35 ml fresh perfusate containing vehicle only (control), the complex I inhibitor rotenone (20 μM) or rotenone (20 μM) + CoQ_1 (50 μM), or CoQ_1 alone (50 μM). Alternatively, the complex I inhibitor piericidin A (1 μM) was used in place of rotenone. With the reservoir stirring continuously, the pump was restarted, the first 10 ml of venous effluent was discarded, and the remaining perfusate was recirculated through the pulmonary circulation. After 10 min of recirculation P_v was raised to ~5 cm H_2O (zone III conditions) and the lung was perfused for 20 min. At the end of the 20 min, 1 ml of perfusate was collected from the stirred reservoir, flash frozen in liquid N_2 and stored at −80°C for measurements of lactate and pyruvate. Then, P_v was raised to ~13.5 cm H_2O and perfusion continued for an additional 10 min. These step changes in pressure were more than adequate to allow appropriate measure of K_f [22].

K_f was determined by dividing the rate of weight gain measured 10 minutes after increasing P_v from 5 to 13.5 cm H_2O by the change in pulmonary capillary pressure (P_c), the latter estimated as (P_a + P_v)/2. The rate of weight gain at $P_v \cong 13.5$ cm H_2O was corrected for any nonisogravimetric weight gain during the $P_v \cong 5$ cm H_2O period. K_f was normalized per 1 gram dry lung weight.

Statistics

A one- way ANOVA with multiple comparisons was carried out by the Waller-Duncan k-ratio t test method using SAS 9.2. [39]. The Waller-Duncan test is an adaptive test which uses a very conservative (as large as the Bonferroni) critical value if the overall groups p value is near 0.05 and a much smaller critical value (nearly Fisher's critical value) when the overall test is quite significant, thus showing that there are many differences to detect. It provides more clarity and power to detect differences between groups than methods that are static in cutoff. In addition, since many of the variables have different standard deviations in the groups, a log transformation of each data

point was used to stabilize the variance – a key assumption for an ANOVA. The results were then transformed back to the original scale.

Results

The effects of rotenone alone (20 M) or rotenone + CoQ_1 (50 µM) on lung ATP, ADP and AMP content are shown in Table 1. Rotenone depressed lung ATP content and elevated ADP and AMP. When CoQ_1 was also present (rotenone + CoQ_1), ATP, ADP and AMP levels were indistinguishable from those in the untreated control lungs, demonstrating that CoQ_1 prevented the rotenone-induced lung ATP depletion and adenine nucleotide imbalance. In contrast, the effects of rotenone on lung ATP, ADP and AMP could not be overcome by CoQ_1 when inhibitors of NQO1 (dicumarol) or complex III (antimycin A) were also present (Table 1). The requirement for active NQO1 and complex III for maintenance of lung ATP is consistent with a CoQ_1 mechanism involving complex I bypass, wherein CoQ_1 is reduced to CoQ_1H_2 by NQO1 and the CoQ_1H_2 produced is reoxidized at complex III, as depicted in Scheme 1C**.**

Treatment	n	ATP	ADP	AMP	ATP + ADP + AMP
Vehicle Control	7	5.66 ± 0.46 [b]	1.17 ± 0.14 [b,c]	0.31 ± 0.06 [c]	7.15 ± 0.33 [b]
Rotenone	8	2.34 ± 0.15 [c]	1.83 ± 0.09 [a]	1.73 ± 0.29 [b]	5.90 ± 0.37 [c]
Rotenone + CoQ$_1$	7	5.38 ± 0.29 [b]	1.22 ± 0.07 [b]	0.30 ± 0.04 [c]	6.90 ± 0.35 [b,c]
CoQ$_1$	4	7.72 ± 0.36 [a]	0.93 ± 0.05 [c]	0.14 ± 0.04 [d]	8.79 ± 0.34 [a]
Rotenone + CoQ$_1$ + Dicumarol	5	1.23 ± 0.09 [e]	1.58 ± 0.04 [a]	3.12 ± 0.22 [a]	5.93 ± 0.35 [c]
Rotenone + CoQ$_1$ + Antimycin A	5	1.68 ± 0.05 [d]	1.58 ± 0.04 [a]	2.84 ± 0.30 [a]	6.10 ± 0.23 [c]

Table 1 **Rat lung tissue adenine nucleotide content (µmol·gram^{-1} dry lung) after 15 min of perfusion with the experimental treatments in Protocol 1 studies**

The values are means ± SE. Statistical analysis was carried out using ANOVA, with multiple comparisons made using the Waller-Duncan k-ratio t-test. Means with the same letter designations are in the same group and not significantly different ($p > 0.05$). Means with two letters are not different from either group. Means with different letter designations are in different groups and are significantly different from each other ($p < 0.05$).

Figures 1A - C show the lung ADP:ATP ratios, AMP:ATP ratios and energy charges calculated from the Table 1 data, where energy charge is defined as (ATP + ½ ADP)/(AMP + ADP + ATP). As compared to control, rotenone increased the ADP:ATP and AMP:ATP ratios and depressed the energy charge. When CoQ$_1$ was present along with rotenone, the ADP:ATP and AMP:ATP ratios and the energy charge were not detectably different from controls. When the NQO1 or complex III inhibitors, dicumarol or antimycin A, respectively, were included with CoQ$_1$ + rotenone, they blocked the ability of CoQ$_1$ to prevent the rotenone-induced disruption of adenine nucleotide balance, as exemplified in Figures 1A - C.
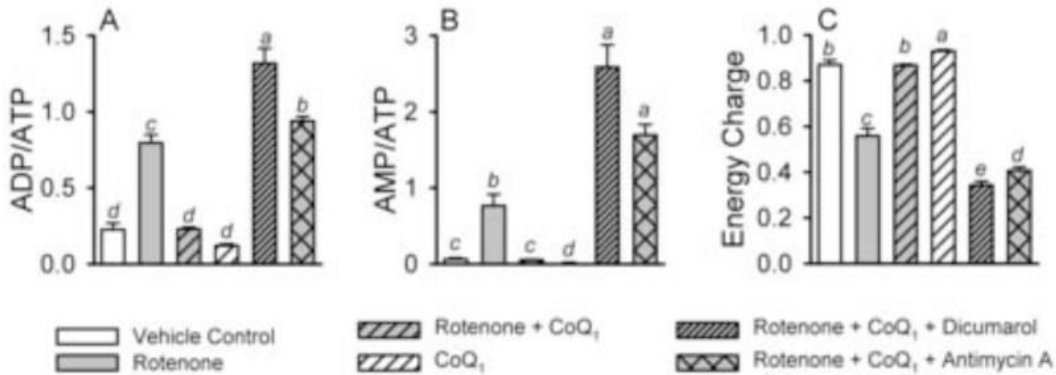
Figure 1 **Rat lung tissue ADP/ATP ratios (A), AMP/ATP ratios (B) and energy charges (C) after 15 min of perfusion with experimental treatments** The ratios and energy charges (mean ± SE) were calculated from the individual lung data used to calculate the mean values in Table 1. Energy charge was calculated as (ATP + ½ ADP)/(ATP + ADP + AMP). Statistics were carried out as described in Table 1, wherein means with the same letter designation are not significantly different from each other ($p < 0.05$); means with different letters are significantly different.

Figure 2 shows the fractional ATP, ADP or AMP concentrations vs the energy charges calculated for each of the 36 individual lungs used to obtain the mean values in Table 1. This representation emphasizes the wide range in lung energy charges produced by the experimental treatments. The solid lines represent the theoretically predicted proportions of ATP:ADP:AMP at any given energy charge under the assumption that the adenylate kinase reaction is a key factor regulating the equilibrium levels [34, 35] (See Appendix).
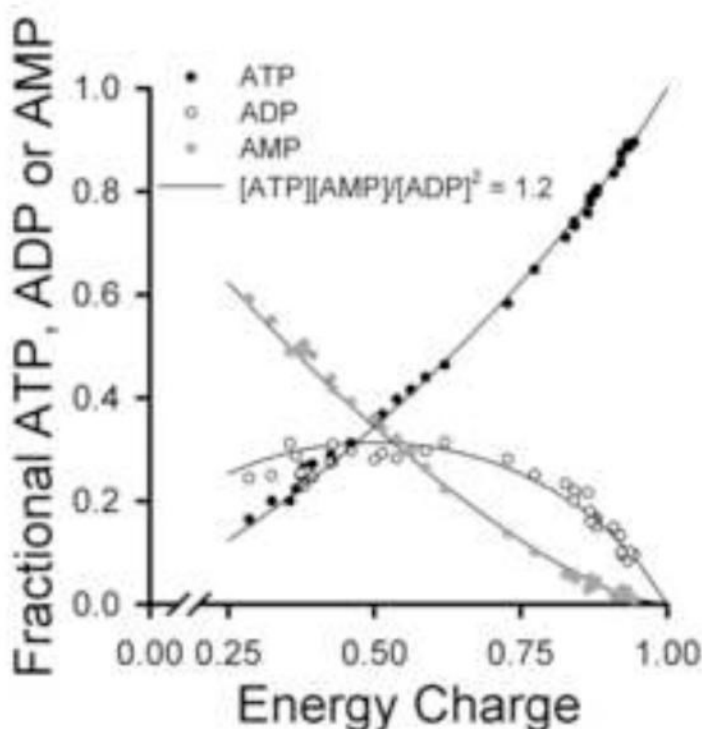
Figure 2 **Lung tissue fractional concentrations of ATP, ADP and AMP vs energy charge for the experimental treatments in Protocol 1 studies**
The symbols are the fractional adenine nucleotide values calculated from individual lung adenine nucleotide measurements that make up the mean values in Table 1 (n = 36). Energy charge was calculated as described in the Figure 1 legend. The solid lines show the theoretical proportions of ATP, ADP and AMP present at the indicated energy charge if the adenylate kinase equilibrium $[ATP][AMP]/[ADP]^2 = 1.2$ was controlling the relative amounts of the adenine nucleotides [35].

Table 2 shows the effects of the treatment conditions on lung lactate and pyruvate production, and the total lactate + pyruvate levels. As compared to control, rotenone increased lung lactate generation with no detectable effect on pyruvate, suggesting activation of glycolysis as a compensatory response to complex I blockade [40]. Then, as compared to rotenone alone, CoQ_1 + rotenone decreased lactate levels and increased pyruvate levels (Table 2), implying that CoQ_1 tends to dampen the impact of rotenone to activate glycolysis. The increase in pyruvate is apparent for every Table 2 treatment containing CoQ_1. The effect of CoQ_1 to mitigate the rotenone-induced increase in glycolytic activity, as reflected by lactate levels, was effectively blocked by dicumarol and antimycin A (Table 2). Figure 3 shows the negative correlation between lactate levels (i.e., glycolytic

activity) and energy charge across the treatment groups, suggesting that activation of glycolysis could not fully compensate for the energy deficit induced by complex I blockade.
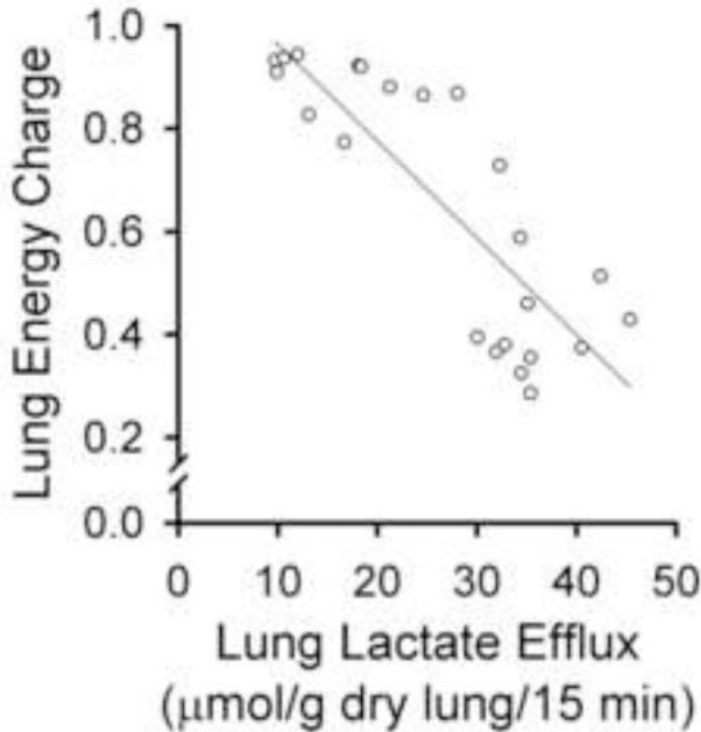

Figure 3 **Lung perfusate lactate vs lung tissue energy charge in Protocol 1 studies**

Each symbol represents the lactate level for an individual lung (from Tables 1 and and2),2), plotted vs the energy charge calculated for the same lung. Pearson Product Moment Correlation r = 0.837, p<0.01.

Treatment	n	Lactate	Pyruvate	Lactate + Pyruvate
Vehicle Control	4	12.36 ± 1.64 [c]	0.88 ± 0.11 [d]	13.24 ± 1.66 [c]
Rotenone	4	38.62 ± 3.14 [a]	0.87 ± 0.14 [d]	39.49 ± 3.12 [a]
Rotenone + CoQ_1	3	24.64 ± 1.96 [b]	2.58 ± 0.20 [a]	27.23 ± 1.92 [b]
CoQ_1	4	14.77 ± 2.02 [c]	2.12 ± 0.18 [a,b]	16.90 ± 2.08 [c]
Rotenone + CoQ_1 + Dicumarol	4	34.31 ± 0.81 [a]	1.70 ± 0.26 [b,c]	36.01 ± 0.97 [a]
Rotenone + CoQ_1 + Antimycin A	4	34.63 ± 2.22 [a]	1.42 ± 0.06 [c]	36.05 ± 2.19 [a]

Table 2 Lung lactate and pyruvate production over the 15 min treatment periods ($\mu mol \cdot 15\ min^{-1} \cdot gram^{-1}$ dry lung) in Protocol 1 studies

Measurements were made in pulmonary venous effluent samples of a subset of lungs in Table 1. The values are means ± SE. Statistical analysis was carried out as described in Table 1. Means with the same letter designation are in the same group and not significantly different ($p > 0.05$); means with different letter designations are in different groups and significantly different from each other ($p < 0.05$).

Figure 4 shows the effect of the treatment conditions on lung tissue lactate and pyruvate levels expressed as the lactate/pyruvate ratio, as an index of cytosolic $NADH/NAD^+$ status. Rotenone substantially increased the ratio as compared to control, and when CoQ_1 was added with rotenone, the ratio was normalized. However, with CoQ_1 alone, the ratio was actually lower than control, a reflection of the general CoQ_1 impact on pyruvate levels seen in Table 2. This CoQ_1 effect also comes into play when dicumarol or antimycin are added, wherein we might expect either to more convincingly block the mitigating effect of CoQ_1 on the rotenone-induced increase in lactate/pyruvate ratio. Table 3 shows that despite the large effect rotenone had on the lactate/pyruvate ratio, it had no detectable impact on whole lung glutathione redox status (GSH/GSSG).
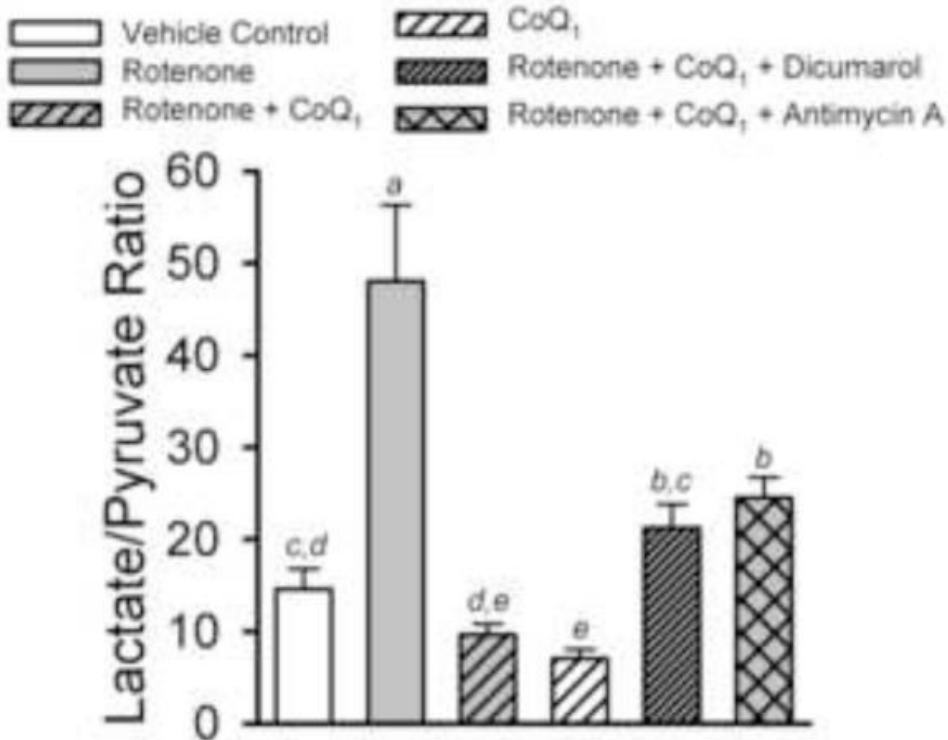
Figure 4 **Lung perfusate lactate/pyruvate ratios produced by the treatments in Protocol 1 studies**

The lactate/pyruvate ratios (mean ± SE) were calculated from the individual lung lactate and pyruvate data used to calculate the mean values in Table 2. Statistical analysis was carried out as described in Table 1. Means with the same letter designation are not significantly different (p>0.05); means with different letter designations are significantly different from each other (p<0.05).

Treatment	n	GSH	GSSG	GSH + GS	GSH/GSSG
Vehicle Control	7	10.71 ± 0.77	0.36 ± 0.05	11.44 ± 0.84	32.61 ± 4.40
Rotenone	8	9.73 ± 0.69	0.34 ± 0.03	10.35 ± 0.70	30.76 ± 3.94

Table 3 **Lung tissue reduced (GSH) and oxidized (GSSG) glutathione after 15 min perfusion with rotenone ($\mu mol \cdot gram^{-1}$ dry lung) in Protocol 1 studies**

Values are means ± SE. There were no statistically significant differences (t-test, p>0.05).

Table 4 shows that there were no statistically significant effects of Protocol 1 study conditions or treatments on lung wet-dry weight ratios or pulmonary arterial perfusion pressures, and thus no detectable overt, non-specific lung injury.

Treatment	n	Body Weight (g)	Lung Wet to Dry Weight Ratio	Pulmonary Arterial Pressure (cm H_2O)
Vehicle Control	7	362.9 ± 27.6	5.87 ± 0.24	7.3 ± 0.9
Rotenone	8	362.4 ± 31.8	5.83 ± 0.13	6.8 ± 0.5
Rotenone + CoQ$_1$	7	387.7 ± 41.6	5.67 ± 0.20	6.9 ± 0.7
CoQ$_1$	4	322.0 ± 7.1	5.29 ± 0.07	6.6 ± 0.4
Rotenone + CoQ$_1$ + Dicumarol	5	326.4 ± 6.4	5.88 ± 0.14	6.4 ± 0.3
Rotenone + CoQ$_1$ + Antimycin A	5	316.6 ± 3.4	5.55 ± 0.12	6.3 ± 0.7

Table 4 **Body weights, lung wet:dry weight ratios and pulmonary arterial (perfusion) pressures for Protocol 1 studies**

Data are means ± SE. There were no statistically significant differences between parameter values in the different study groups ($p > 0.05$).

The isolated perfused rat lung was treated with the complex I inhibitor rotenone. Rotenone depressed lung ATP and energy charge with no detectable impact on GSH:GSSG. Rotenone increased the pulmonary endothelial filtration coefficient (K_f). Coenzyme Q$_1$ largely prevented the effects of rotenone in the lung.

The CoQ$_1$ mechanism was via complex I bypass and restoration of lung ATP generation.

Figure 5 shows the impact of rotenone on pulmonary endothelial permeability, in the absence or presence of CoQ_1, measured as K_f in Protocol 2 studies. We note that conditions were met for accurate estimation of K_f [22]: step changes in pressure were more than adequate and the treatments had no detectable effects on hemodynamic parameters (P_a, P_v, pulmonary vascular resistance or pulmonary capillary pressure, data not shown). K_f was 3.6 fold higher in rotenone-treated than control lungs ($p < 0.05$). CoQ_1 prevented the rotenone-induced increase in K_f, without having a detectable impact on its own (Figure 5). Further, as shown in Figure 6, the Protocol 2 study conditions used to determine K_f did not in and of themselves influence the impact of the treatment conditions on lung cytosolic redox status, as reflected in the lactate:pyruvate ratios, since these were reasonably similar to those obtained in the Protocol 1 studies (Figure 4).
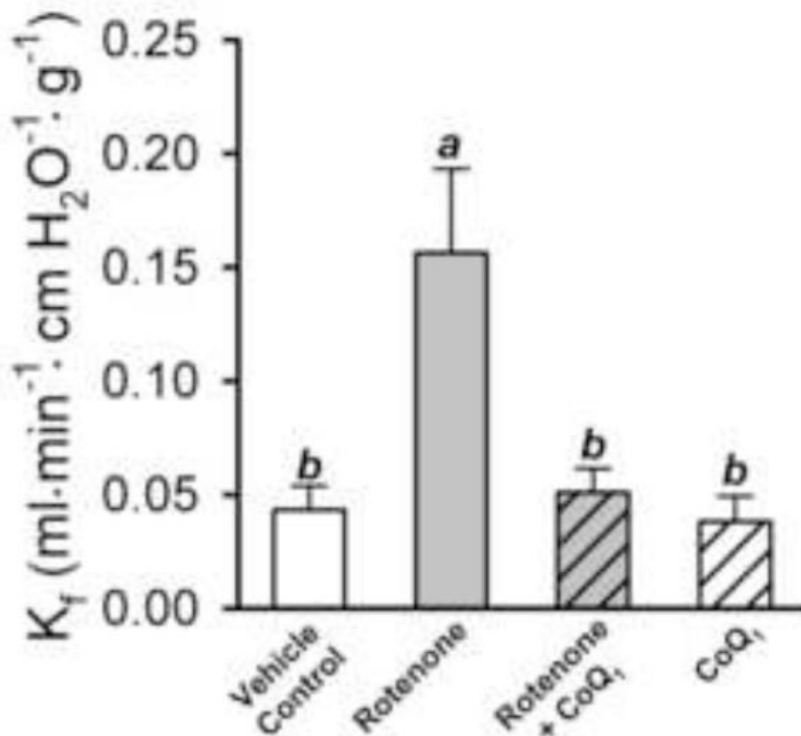

Figure 5 **Effect of rotenone and CoQ_1 on the filtration coefficient (K_f) in rat lung in Protocol 2 studies**
The bars represent the means ± SE for K_f measured in vehicle control (n = 13), rotenone (n = 6), rotenone + CoQ_1 (n = 6), or CoQ_1 (n = 7) treated lungs. Means with the same letter designation are not significantly different (p>0.05); means with different letter designations are significantly different from each other (p<0.05).

Figure 6 **Lung perfusate lactate/pyruvate ratios in lungs undergoing K_f procedure in Protocol 2 studies**

The ratios (mean ± SE) obtained from Figure 5 studies, including vehicle control (n = 13), rotenone (n = 6), rotenone + CoQ_1 (n = 6) and CoQ_1 only (n = 7) treated lungs. Statistical analysis was carried out as described in Table 1. Means with the same letter designation are not significantly different (p>0.05); means with different letter designations are significantly different from each other (p<0.05).
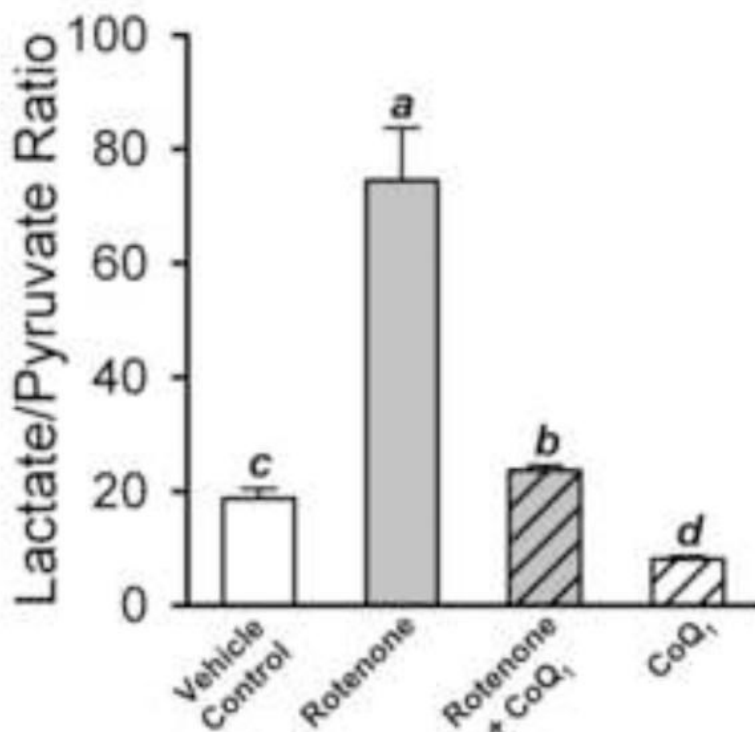
Finally, Figure 7 shows that an alternative complex I inhibitor, piericidin A, produced qualitatively similar effects to rotenone on the K_f and lactate:pyruvate ratios in Protocol 2 studies.
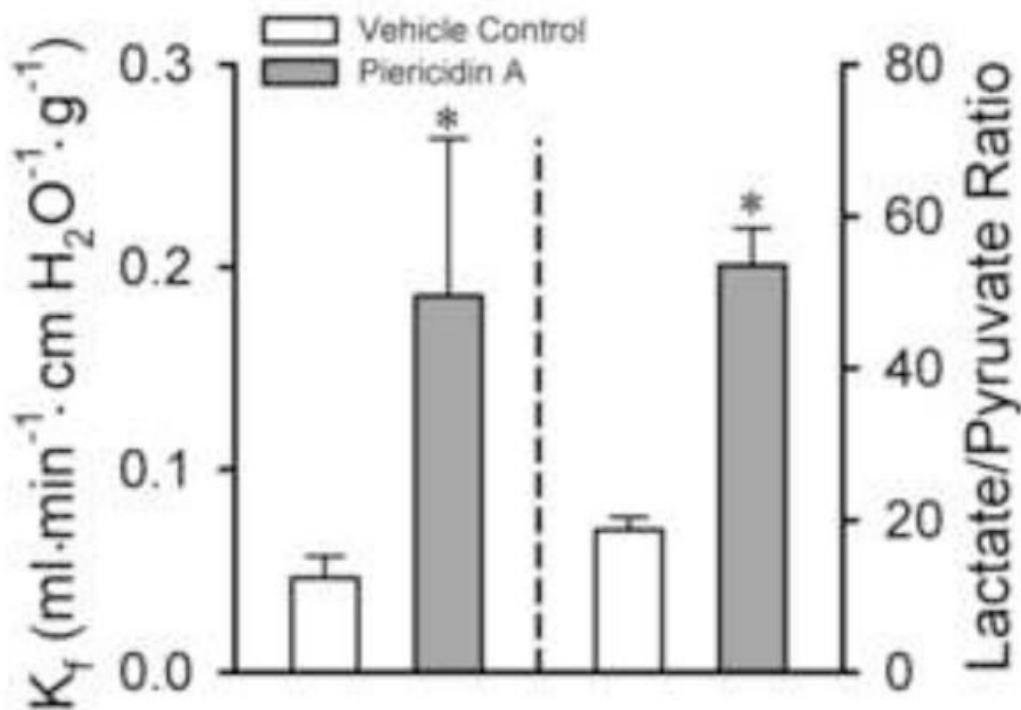
Figure 7 **Effect of the complex I inhibitor piericidin A on K_f and lung perfusate lactate/pyruvate ratios in Protocol 2 studies**
The bars represent the means ± SE for K_f measured in vehicle controls (n = 13) or piericidin A (n = 7) treated lungs. * Significantly different from control (p<0.05; t-test).

Discussion

The study demonstrates that rotenone-induced blockade of mitochondrial electron transport complex I in the isolated perfused rat lung resulted in ATP depletion and depression of the adenylate energy charge. Rotenone also increased perfusate lactate levels, the lactate:pyruvate ratio, and pulmonary vascular endothelial permeability, measured as K_f. A second complex I inhibitor, piericidin A, qualitatively reproduced the impact of rotenone on K_f and the lactate:pyruvate ratio.

The quinone CoQ_1 largely prevented the impact of rotenone on lung tissue ATP levels, energy charge and lactate production. The ability of CoQ_1 to prevent the effects of rotenone on these biochemical parameters depended on both NQO1 and complex III activities. In separate studies, CoQ_1 also blocked the rotenone-induced increase in

K_f. Under the assumption that this CoQ_1 effect on K_f involves restoration of mitochondrial bioenergetics, reflected as ATP generation, and thus would also depend on NQO1 and complex III activities, the study implicates a CoQ_1 mechanism involving a cytosolic-mitochondrial electron shuttle that bypasses complex I to restore mitochondrial electron transport by transfer of electrons to complex III. This sequence of quinone:hydroquinone redox reactions with restoration of mitochondrial respiration in pharmacological or genetic complex I dysfunction has been reported in the isolated perfused rat lung using duroquinone, and by others in various cell and isolated mitochondrial preparations using a range of quinones [26-29]. However, to our knowledge, the present findings provide the first evidence showing bioenergetic and functional protection afforded by a quinone in a complex I activity-deficient intact organ preparation and implicating complex I bypass as the mechanism,.

In our study, the read-out for blockade of mitochondrial electron transport was ATP production and the adenylate energy charge. The energy charge vs fractional ATP, ADP and AMP relationships shown in Figure 2 suggest that the lung is a highly energized and metabolically active organ, able to maintain a predictable ATP:ADP:AMP equilibrium across a range of bioenergetic manipulations, consistent with previous studies [1, 9, 41]. The solid lines in Figure 2 represent the theoretically predicted proportions of ATP:ADP:AMP at any given energy charge. This prediction is based on the assumption that the adenylate kinase reaction is a key factor regulating the equilibrium levels [34, 35] (see Appendix). Insofar as adenylate kinase has been implicated as a key reaction regulating energy balance and ATP availability under conditions of increased stress, represented here by rotenone treatment, the close adherence of the data to the prediction is consistent with the concept of this enzyme as such a regulatory factor, and suggest that the treatments did not exert non-specific effects on adenylate kinase and/or other components involved in this process [42].

The impact of rotenone on lung perfusate lactate and pyruvate levels implies that complex I blockade evoked a compensatory increase in glycolytic activity, as in other lung studies using rotenone or other mitochondrial inhibitors [1, 23, 40, 43]. Accordingly, the rotenone effect on the lactate/pyruvate ratio is consistent with

inhibition of mitochondrial electron transport [23]. Of course, like the adenine nucleotide measurements, perfusate lactate and pyruvate levels represent the whole lung. Whereas the relative contribution arising from any given lung cell type or tissue compartment is unknown, and even the relative contribution of mitochondrial vs glycolytic energy production in the in situ pulmonary endothelium is debated, we would expect that pulmonary endothelial cells contribute substantially to the net effect based on their contribution to total lung cell volume. Nevertheless, glycolysis could not fully compensate for the adenylate energy imbalance caused by complex I blockade, nor could it overcome the functional consequence of complex I blockade, i.e., pulmonary endothelial hyperpermeability. This observation is consistent with a previous study showing that glycolysis was not required to maintain pulmonary endothelial-epithelial barrier function in the perfused rabbit lung [40]. In contrast to the intact lung, pulmonary endothelial cells in culture required simultaneous inhibition of glycolytic and mitochondrial ATP generation to evoke a permeability response [44]. The implication is that the relative contribution of mitochondrial bioenergetic function to pulmonary endothelial barrier integrity is more dominant in the intact lung than in cell culture conditions.

Whereas CoQ_1 prevented the rotenone-induced depression in ATP, and tended to dampen the impact of rotenone on glycolysis (as reflected in lactate levels), the elevated pyruvate generation whenever CoQ_1 was present suggests that it may have done so at the expense of cytosolic NADH, as a source of reducing equivalents for reduction of both CoQ_1 and pyruvate, the latter via the lactate dehydrogenase reaction. Then the CoQ_1-induced effect on pyruvate could be explained as competition for NADH. However, although we did not carry out a flux analysis, the observation that the CoQ_1-induced increases in pyruvate account for only $\sim 2 - 4\%$ of the total lactate + pyruvate suggests an additional or supplementary electron donor pathway for CoQ_1 reduction. Our previous observations implicate pentose phosphate pathway generated NADPH, which we showed to be the predominant source of reducing equivalents for NQO1-catalyzed duroquinone reduction in pulmonary endothelial cells in culture [33]. We also demonstrated that the majority of CoQ_1 reduction on passage through the rat pulmonary circulation in the presence of rotenone is via NQO1 [2]. Under the assumption that NADPH would also be a

dominant electron donor for NQO1-catalyzed CoQ_1 reduction in the rat lung, quinone activation of the pentose phosphate pathway would generate the NADPH to reduce CoQ_1 (via the oxidative branch) and explain a CoQ_1 effect to increase glycolytic intermediates (via the non-oxidative branch). Then the net result of CoQ_1 would be enhanced ATP generation via both mitochondrial and glycolytic pathways.

Inhibition of mitochondrial electron transport with rotenone or piericidin A has been implicated in reactive oxygen species (ROS) generation in some cell types and sub-cellular preparations [45-48]. However, in the lung and pulmonary endothelial cells, several reports indicate that acute rotenone treatment actually suppresses ROS generation induced by various stimuli, including elevated pulmonary capillary pressure or hyperoxia [49-53]. We did not measure ROS generation per se, but the rotenone treatment in the present study did not deplete GSH or alter the GSH:GSSG ratio in whole lung tissue, suggesting that if excessive ROS production occurred, it did not cause global, overt oxidative stress. However, we acknowledge that the GSH:GSSG ratio in total lung tissue may not reveal mild or compartmentalized ROS generation that could initiate a focal Ca^{2+}-dependent hyperpermeability response [54]. In that case, CoQ_1 mitigation of the rotenone-induced permeability response might be attributed to the antioxidant activity of CoQ_1H_2. However, we do not favor this interpretation, as it does not account for the observation that complex III inhibition blocks the mitigating effect of CoQ_1 on adenine nucleotide balance under conditions in which CoQ_1H_2 would continue to be generated via NQO1.

Another potential mechanism by which rotenone could impact pulmonary endothelial permeability is via direct disruption of microtubule assembly, wherein microtubules are an essential cytoskeletal element influencing permeability of cultured endothelial cell monolayers [55-58]. Whether rotenone is acting as a microtubule disrupter in the present study was not evaluated. However, insofar as CoQ_1 protected against the impact of rotenone on K_f, and if anything, certain other quinones cause microtubule disruption, a CoQ_1 mechanism involving direct microtubule stabilization seems unlikely [59].

We have interpreted the data from the perspective that K_f reflects primarily endothelial permeability in the isolated lung. This interpretation must take into account the recognition of lung endothelial heterogeneity, that is, the notion that endothelium in lung extra-alveolar vessels and the alveolar septal compartment display distinct metabolic and permeability-responsive phenotypes [60]. For example, lung microvascular endothelial cells, at least in cell culture, are more glycolytic than those derived from the pulmonary artery [61]. The more glycolytic phenotype may confer a relative insensitivity to mitochondrial blockade, relegating the increased permeability response to the larger extra-alveolar vessels. Nevertheless, we found that glycolysis, no matter how robust, failed to fully compensate for the rotenone effects on energy charge or pulmonary endothelial permeability.

A straightforward explanation of the rotenone-induced increase in K_f is that disruption of mitochondrial bioenergetic function, reflected as ATP depletion, impairs the pulmonary endothelial permeability response, an effect mitigated by CoQ_1. Several potential mechanisms should be considered here. First, ATP could be required as the energy source for repletion of intracellular Ca^{2+} stores that drive store operated channel-mediated pulmonary endothelial permeability responses [62]. If true, ATP depletion would preferentially impact permeability in extra-alveolar vessels and lead to perivascular cuffing rather than alveolar flooding. Yet we observed that lungs treated with rotenone or piericidin A tended to develop frank alveolar flooding by the end of the perfusion period. Second, viewing ATP depletion in a broader sense, as a biomarker of mitochondrial dysfunction, other possibilities arise, including impaired mitochondrial Ca^{2+} handling [62-64]. While a role for mitochondrial Ca^{2+} has not been evaluated in the context of pulmonary endothelial barrier function, it has been implicated in transducing pressure-induced pro-inflammatory responses in lung venular capillaries [53]. If mitochondrial Ca^{2+} signaling is a mechanism of pulmonary endothelial barrier dysfunction, we predict that the effect would not be restricted to a specific lung vascular compartment. Finally, K_f may also be influenced by depressed activity of the alveolar epithelial Na^+/K^+-ATPase, wherein tight junction structure and permeability are highly ATP-dependent in alveolar and other epithelial cells [65-67]. However, while rotenone exposure mimics the hyperoxia-induced decrease in complex I activity observed

in rats breathing 85% O_2 for 48 hours, exposure to the same sub-lethal oxygen tension, albeit for longer time courses, is associated with increased trans-epithelial sodium transport, and thus increased alveolar fluid clearance [68]. Further observations that alveolar epithelial Na^{+2} transport can be supported by glycolysis in the presence of mitochondrial inhibitors, including rotenone, has actually led others to conjecture that the pulmonary endothelium is the site of barrier failure in mitochondrial insufficiency [43]. In light of these studies, the implication is that the pulmonary endothelium is also a predominant site of the hyperoxia-induced increase in K_f observed in the rabbit lung [25]. Nonetheless, our conclusion that complex I bypass affords significant protection against rotenone-induced barrier dysfunction in lung remains valid regardless of whether the endothelium, epithelium or both provide the main target.

Conclusion

Mitochondrial bioenergetic dysfunction, reflected as ATP depletion, and/or decreased activity of electron transport complexes or other mitochondrial components have been reported in various forms of experimental and clinical lung disease, including hyperoxia, phosgene- or paraquat-induced lung injury, ischemia reperfusion injury, in lung preservation for transplantation and in chronic obstructive pulmonary disease [9, 16-21]. One aspect of such dysfunction is a deficiency in movement of reducing equivalents through the mitochondrial electron transport chain and ATP depletion. Amphipathic CoQ_{10} homologs and analogs (e.g., CoQ_1) restore mitochondrial function and ATP generation by shuttling reducing equivalents from the cytosol to the mitochondria [28-30, 32]. This mechanism provides one basis for use of quinones in treating patients with neurological and other disorders associated with genetic mitochondrial deficiencies [31]. The present study demonstrates that CoQ_1 prevents energy charge depletion and pulmonary endothelial hyperpermeability evoked by complex I blockade in the isolated perfused rat lung, and provides evidence that the impact on energy charge is via a cytosolic-mitochondrial electron shuttle. The implication is that certain quinones may also be beneficial in protection of the lung from pulmonary edema associated with acute lung injury, when the injury involves mitochondrial dysfunction.

Supplementary Material

Appendix:

Adenylate kinase catalyzes the following reaction:

$$ATP + AMP \underset{k_{-1}}{\overset{k_1}{\rightleftharpoons}} 2ADP$$
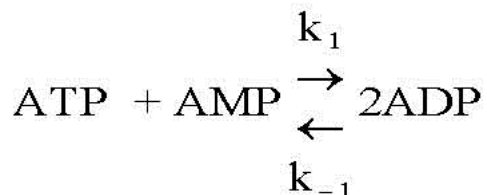
Using mass action:

$$\text{Dissociation rate constant} = K = \frac{k_{-1}}{k_1} = \frac{[ATP][AMP]}{[ADP]^2} \tag{1}$$

$$\text{Energy charge} = EC = \frac{[ATP] + \dfrac{[ADP]}{2}}{[ATP] + [ADP] + [AMP]} \tag{2}$$

$$\text{Assuming that } [ATP] + [ADP] + [AMP] = \alpha = 1 = \text{constant}, \tag{3}$$

Then using algebraic manipulation of equations (1-2), one could show that:

$$[ADP] = \frac{-0.5 + \sqrt{(0.5)^2 + 4\left(K - 0.25\right)\left(EC - EC^2\right)}}{2\left(K - 0.25\right)} \tag{4}$$

Thus, for a given EC and K values, equation (4) can used to determine [ADP]. Knowing [ADP], then [ATP] and [AMP] are determined from equation (2) and equation (3), respectively.

Acknowledgements

Footnotes

Publisher's Disclaimer: This is a PDF file of an unedited manuscript that has been accepted for publication. As a service to our customers we are providing this early version of the manuscript. The manuscript will undergo copyediting, typesetting, and review of the resulting proof before it is published in its final citable form. Please note that during the production process errors may be discovered which could affect the content, and all legal disclaimers that apply to the journal pertain.

References

[1] Fisher AB. Intermediary metabolism of the lung. Environ.Health Perspect. 1984;55:149–158.

[2] Audi SH, Merker MP, Krenz GS, Ahuja T, Roerig DL, Bongard RD. Coenzyme Q_1 redox metabolism during passage through the rat pulmonary circulation and the effect of hyperoxia. J Appl Physiol. 2008;105:1114–1126.

[3] Gardner PR, Nguyen DD, White CW. Aconitase is a sensitive and critical target of oxygen poisoning in cultured mammalian cells and in rat lungs. Proc Natl Acad Sci U.S.A. 1994;91:12248–12252.

[4] Hashizume M, Mouner M, Chouteau JM, Gorodnya OM, Ruchko MV, Potter BJ, Wilson GL, Gillespie MN, Parker JC. Mitochondrial targeted DNA repair enzyme 8-oxoguanine DNA glycosylase 1 protects against ventilator induced lung injury in intact mice. Am J Physiol Lung Cell Mol Physiol. 2012;304:L287–L297.

[5] Bongard RD, Myers CR, Lindemer BJ, Baumgardt S, Gonzalez FJ, Merker MP. Coenzyme Q_1 as a probe for mitochondrial complex I activity in the intact perfused hyperoxia-exposed wild-type and *Nqo1*-null mouse lung. Am J Physiol Lung Cell Mol Physiol. 2012;302:L949–L958.

[6] Chuang GC, Yang Z, Westbrook DG, Pompilius M, Ballinger CA, White CR, Krzywanski DM, Postlethwait EM, Ballinger SW. Pulmonary ozone exposure induces vascular dysfunction, mitochondrial damage, and

atherogenesis. Am J Physiol Lung Cell Mol Physiol. 2009;297:L209–L216.

[7] Xu W, Koeck T, Lara AR, Neumann D, DiFilippo FP, Koo M, Janocha AJ, Masri FA, Arroliga AC, Jennings C, Dweik RA, Tuder RM, Stuehr DJ, Erzurum SC. Alterations of cellular bioenergetics in pulmonary artery endothelial cells. Proc Natl Acad Sci U.S.A. 2007;104:1342–1347.

[8] Qiu W, Gu H, Zheng L, Zhou J, Chen D, Chen Y. Pretreatment with edaravone reduces lung mitochondrial damage in an infant rabbit ischemia-reperfusion model. J Pediatr Surg. 2008;43:2053–2060.

[9] De Leyn PR, Lerut TE, Schreinemakers HH, Van Raemdonck DE, Mubagwa K, Flameng W. Effect of inflation on adenosine triphosphate catabolism and lactate production during normothermic lung ischemia. Ann Thorac Surg. 1993;55:1073–1078.

[10] Sommer SP, Sommer S, Sinha B, Wiedemann J, Otto C, Aleksic I, Schimmer C, Leyh RG. Ischemia-reperfusion injury-induced pulmonary mitochondrial damage. J Heart Lung Transplant. 2011;30:811–818.

[11] Fukushima T, Gao T, Tawara T, Hojo N, Isobe A, Yamane Y. Inhibitory effect of nicotinamide to paraquat toxicity and the reaction site on complex I. Arch Toxicol. 1997;71:633–637.

[12] Soulitzis N, Neofytou E, Psarrou M, Anagnostis A, Tavernarakis N, Siafakas N, Tzortzaki EG. Downregulation of lung mitochondrial prohibitin in COPD. Resp Med. 2012;106:954–961.

[13] Sommer SP, Sommer S, Sinha B, Leyh RG. Glycine preconditioning to ameliorate pulmonary ischemia reperfusion injury in rats. Interact Cardiovasc Thorac Surg. 2012;14:521–525.

[14] D'Armini AM, Tom EJ, Roberts CS, Henke DC, Lemasters JJ, Egan TM. When does the lung die? Time course of high energy phosphate depletion and relationship to lung viability after "death" J Surg Res. 1995;59:468–474.

[15] Qin XJ, Li YN, Liang X, Wang P, Hai CX. The dysfunction of ATPases due to impaired mitochondrial respiration in phosgene-induced pulmonary edema. Biochem Biophys Res Commun. 2008;367:150–155.

[16] Fukuse T, Hirata T, Ueda M, Nakamura T, Kawashima M, Hitomi S, Wada H. Energy metabolism and mitochondrial damage during pulmonary preservation. Transplant Proc. 1999;31:1937–1938.

[17] Hirata T, Fukuse T, Nakamura T, Ueda M, Kawashima M, Hitomi S, Wada H. Reperfusion lung injury after cold preservation correlates with decreased levels of intrapulmonary high-energy phosphates. Transplantation. 2000;69:1793–1801.

[18] Aggarwal S, Dimitropoulou C, Lu Q, Black SM, Sharma S. Glutathione supplementation attenuates lipopolysaccharide-induced mitochondrial dysfunction and apoptosis in a mouse model of acute lung injury. Front Physiol. 2012;3:161.

[19] Akai M, Ishizaki T, Matsukawa S, Shigemori K, Miyamori I. Leukotoxin (9, 10-epoxy-12-octadecenoate) impairs energy and redox state of isolated perfused rat lung. Free Radic Biol Med. 1998;25:596–604.

[20] Islam MN, Das SR, Emin MT, Wei M, Sun L, Westphalen K, Rowlands DJ, Quadri SK, Bhattacharya S, Bhattacharya J. Mitochondrial transfer from bone-marrow-derived stromal cells to pulmonary alveoli protects against acute lung injury. Nat Med. 2012;18:759–765.

[21] Fisher AB, Dodia C, Chander A. Energy dependence of lung phosphatidylcholine biosynthesis studied with CO hypoxia. Am J Physiol. 1985;249:E89–93.

[22] Parker JC, Townsley MI. Evaluation of lung injury in rats and mice. Am J Physiol Lung Cell Mol Physiol. 2004;286:L231–L246.

[23] Bassett DJ, Fisher AB. Metabolic response to carbon monoxide by isolated rat lungs. Am J Physiol. 1976;230:658–663.

[24] Bassett DJ, Fisher AB. Stimulation of rat lung metabolism with 2,4-dinitrophenol and phenazine methosulfate. Am J Physiol. 1976;231:898–902.

[25] Matalon S, Cesar MA. Effects of 100% oxygen breathing on the capillary filtration coefficient in rabbit lungs. Microvasc Res. 1985;29:70–80.

[26] Ernster L, Dallner G, Azzone GF. Differential effects of rotenone and amytal on mitochondrial electron and energy transfer. J Biol Chem. 1963;238:1124–1131.

[27] Audi SH, Bongard RD, Dawson CA, Siegel D, Roerig DL, Merker MP. Duroquinone reduction during passage through the pulmonary circulation. Am J Physiol Lung Cell Mol Physiol. 2003;285:L1116–L1131.

[28] Chan TS, Teng S, Wilson JX, Galati G, Khan S, O'Brien PJ. Coenzyme Q cytoprotective mechanisms for mitochondrial complex I cytopathies involves NAD(P)H: quinone oxidoreductase 1(NQO1) Free Radical Res. 2002;36:421–427.

[29] Erb M, Hoffmann-Enger B, Deppe H, Soeberdt M, Haefeli RH, Rummey C, Feurer A, Gueven N. Features of idebenone and related short-chain quinones that rescue ATP levels under conditions of impaired mitochondrial complex I. PLoS ONE. 2012;7:e36153.

[30] Giorgio V, Petronilli V, Ghelli A, Carelli V, Rugolo M, Lenaz G, Bernardi P. The effects of idebenone on mitochondrial bioenergetics. Biochim Biophys Acta (BBA) - Bioenergetics. 2012;1817:363–369.

[31] Kerr DS. Review of clinical trials for mitochondrial disorders: 1997-2012. Neurotherapeutics. 2013;10:307–319.

[32] Lopez LC, Quinzii CM, Area E, Naini A, Rahman S, Schuelke M, Salviati L, DiMauro S, Hirano M. Treatment of CoQ_{10} deficient fibroblasts with ubiquinone, CoQ analogs, and vitamin C: Time- and compound-dependent effects. PLoS ONE. 2010;5:e11897.

[33] Bongard RD, Lindemer BJ, Krenz GS, Merker MP. Preferential utilization of NADPH as the endogenous electron donor for NAD(P)H:quinone oxidoreductase 1 (NQO1) in intact pulmonary arterial endothelial cells. Free Radic Biol Med. 2009;46:25–32.

[34] Atkinson DE. Energy charge of the adenylate pool as a regulatory parameter. Interaction with feedback modifiers. Biochemistry. 1968;7:4030–4034.

[35] Ballard FJ. Adenine nucleotides and the adenylate kinase equilibrium in livers of foetal and newborn rats. Biochem J. 1970;117:231–235.

[36] Owens C, Belcher R. A colorimetric miro-method for the determination of glutathione. Biochem J. 1965;94:705–711.

[37] Tietze F. Enzymatic method for quantitative determination of nanogram amounts of total and oxidized glutathione: applications to mammalian blood and other tissues. Anal Biochem. 1969;27:502–522.

[38] Griffith OW. Determination of glutathione and glutathione disulfide using glutathione reductase and 2-vinylpyridine. Anal Biochem. 1980;106:207–212.

[39] Waller RA, Duncan DB. A Bayes rule for the symmetric multiple comparison problem. J Amer Statist Assoc. 1969;64:1484–1504.

[40] Bolin R, Guest RJ, Albert RK. Glycolysis is not required for fluid homeostasis in isolated rabbit lungs. J Appl Physiol. 1988;64:2517–2521.

[41] De Leyn P, Lerut T, Schreinemakers H, van Belle H, Lauwerijns J, van Lommel F, Verbeken E, Flameng W. Adenine nucleotide degradation in ischemic rabbit lung tissue. Am J Physiol Lung Cell Mol Physiol. 1993;264:L329–L337.

[42] Janssen E, Terzic A, Wieringa B, Dzeja PP. Impaired intracellular energetic communication in muscles from creatine kinase and adenylate kinase (M-CK/AK1) double knock-out mice. J Biol Chem. 2003;278:30441–30449.

[43] Saumon G, Martet G. v. Effect of metabolic inhibitors on Na^+ transport in isolated perfused rat lungs. Am J Respir Cell Mol Biol. 1993;9:157–165.

[44] Hinshaw DB, Burger JM, Miller MT, Adams JA, Beals TF, Omann GM. ATP depletion induces an increase in the assembly of a labile pool of polymerized actin in endothelial cells. Am J Physiol. 1993;264:C1171–C1179.

[45] Adam-Vizi V. Production of reactive oxygen species in brain mitochondria: contribution by electron transport chain and non-electron transport chain sources. Antioxid Redox Signal. 2005;7:1140–1149.

[46] Radad K, Rausch WD, Gille G. Rotenone induces cell death in primary dopaminergic culture by increasing ROS production and inhibiting mitochondrial respiration. Neurochem Int. 2006;49:379–386.

[47] Barrientos A, Moraes CT. Titrating the effects of mitochondrial complex I impairment in the cell physiology. J Biol Chem. 1999;274:16188–16197.

[48] Fato R, Bergamini C, Bortolus M, Maniero AL, Leoni S, Ohnishi T, Lenaz G. Differential effects of mitochondrial Complex I inhibitors on production of reactive oxygen species. Biochim Biophys Acta. 2009;1787:384–392.

[49] Sanders SP, Zweier JL, Kuppusamy P, Harrison SJ, Bassett DJ, Gabrielson EW, Sylvester JT. Hyperoxic sheep pulmonary microvascular endothelial cells generate free radicals via mitochondrial electron transport. J Clinic Invest. 1993;91:46–52.

[50] Brueckl C, Kaestle S, Kerem A, Habazettl H, Krombach F, Kuppe H, Kuebler WM. Hyperoxia-induced reactive oxygen species formation in pulmonary capillary endothelial cells in situ. Am J Respir Cell Mol Biol. 2006;34:453–463.

[51] Zulueta JJ, Yu FS, Hertig IA, Thannickal VJ, Hassoun PM. Release of hydrogen peroxide in response to hypoxia-reoxygenation: role of and NAD(P)H oxidase-like enzyme in endothelial cell plasma membrane. Am J Respir Cell Mol Biol. 1995;12:41–49.

[52] Ouyang JS, Li YP, Li CY, Cai C, Chen CS, Chen SX, Chen YF, Yang L, Xie YP. Mitochondrial ROS-K$^+$ channel signaling pathway regulated secretion of human pulmonary artery endothelial cells. Free Radic Res. 2012;46:1437–1435.

[53] Ichimura H, Parthasarathi K, Quadri S, Issekutz AC, Bhattacharya J. Mechano-oxidative coupling by mitochondria induces proinflammatory responses in lung venular capillaries. J Clin Invest. 2003;111:691–699.

[54] Hecquet CM, Malik AB. Role of H_2O_2-activated TRPM2 calcium channel in oxidant-induced endothelial injury. J Thromb Haemost. 2009;101:619–625.

[55] Ochoa CD, Alexeyev M, Pastukh V, Balczon R, Stevens T. Pseudomonas aeruginosa exotoxin Y Is a promiscuous cyclase that increases endothelial tau phosphorylation and permeability. J Biol Chem. 2012;287:25407–25418.

[56] Verin AD, Birukova A, Wang P, Liu F, Becker P, Birukov K, Garcia JGN. Microtubule disassembly increases endothelial cell barrier dysfunction: role of MLC phosphorylation. Am J Physiol Lung Cell Mol Physiol. 2001;281:L565–L574.

[57] Choi WS, Palmiter RD, Xia Z. Loss of mitochondrial complex I activity potentiates dopamine neuron death induced by microtubule

dysfunction in a Parkinson's disease model. J Cell Biol. 2011;192:873–882.

[58] Tian X, Tian Y, Sarich N, Wu T, Birukova AA. Novel role of stathmin in microtubule-dependent control of endothelial permeability. FASEB J. 2012;26:3862–3874.

[59] Das A, Chakrabarty S, Choudhury D, Chakrabarti G. 1,4-Benzoquinone (PBQ) induced toxicity in lung epithelial cells is mediated by the disruption of the microtubule network and activation of caspase-3. Chem Res Toxicol. 2010;23:1054–1066.

[60] Wu S, Jian MY, Xu YC, Zhou C, Al-Mehdi AB, Liedtke W, Shin HS, Townsley MI. Ca^{2+} entry via $α_{1G}$ and TRPV4 channels differentially regulates surface expression of P-selectin and barrier integrity in pulmonary capillary endothelium. Am J Physiol Lung Cell Mol Physiol. 2009;297:L650–L657.

[61] Parra-Bonilla G, Alvarez DF, Al-Mehdi AB, Alexeyev M, Stevens T. Critical role for lactate dehydrogenase A in aerobic glycolysis that sustains pulmonary microvascular endothelial cell proliferation. Am J Physiol Lung Cell Mol Physiol. 2010;299:L513–L522.

[62] Townsley MI, King JA, Alvarez DF. Ca^{2+} channels and pulmonary endothelial permeability: Insights from study of intact lung and chronic pulmonary hypertension. Microcirc. 2006;13:725–739.

[63] Demaurex N, Poburko D, Frieden M. Regulation of plasma membrane calcium fluxes by mitochondria. Biochim Biophys Acta. 2009;1787:1383–1394.

[64] Willems PH, Valsecchi F, Distelmaier F, Verkaart S, Visch HJ, Smeitink JA, Koopman WJ. Mitochondrial Ca^{2+} homeostasis in human NADH:ubiquinone oxidoreductase deficiency. Cell Calcium. 2008;44:123–133.

[65] Cavanaugh KJ, Jr., Oswari J, Margulies SS. Role of stretch on tight junction structure in alveolar epithelial cells. Am J Respir Cell Mol Biol. 2001;25:584–591.

[66] Mandel LJ, Doctor RB, Bacallao R. ATP depletion: a novel method to study junctional properties in epithelial tissues. II. Internalization of $Na^+,K(^+)$-ATPase and E-cadherin. J Cell Sci. 1994;107:3315–3324.

[67] Khimenko PL, Barnard JW, Moore TM, Wilson PS, Ballard ST, Taylor AE. Vascular permeability and epithelial transport effects on lung edema formation in ischemia and reperfusion. J Appl Physiol. 1994;77:1116–1121.

[68] Yue G, Matalon S. Mechanisms and sequelae of increased alveolar fluid clearance in hyperoxic rats. Am J Physiol. 1997;272:L407–L412.